



DOI: 10.29026/oea.2020.200013

High-sensitivity distributed dynamic strain sensing by combining Rayleigh and Brillouin scattering

Benzhang Wang[†], Dexin Ba[†], Qi Chu, Liqiang Qiu, Dengwang Zhou and Yongkang Dong*

The phase-sensitive optical time-domain reflectometry (φ -OTDR) is a good candidate for distributed dynamic strain sensing, due to its high sensitivity and fast measurement, which has already been widely used in intrusion monitoring, geophysical exploration, etc. For the frequency scanning based φ -OTDR, the phase change manifests itself as a shift of the intensity distribution. The correlation between the reference and measured spectra is employed for relative strain demodulation, which has imposed the continuous measurement for the absolute strain demodulation. Fortunately, the Brillouin optical time domain analysis (BOTDA) allows for the absolute strain demodulation with only one measurement. In this work, the combination of the φ -OTDR and BOTDA has been proposed and demonstrated by using the same set of frequency-scanning optical pulses, and the frequency-agile technique is also introduced for fast measurements. A 9.9 Hz vibration with a strain range of 500 n ϵ has been measured under two different absolute strains (296.7 $\mu\epsilon$ and 554.8 $\mu\epsilon$) by integrating the Rayleigh and Brillouin information. The sub-micro strain vibration is demonstrated by the φ -OTDR signal with a high sensitivity of 6.8 n ϵ , while the absolute strain is measured by the BOTDA signal with an accuracy of 5.4 $\mu\epsilon$. The proposed sensor allows for dynamic absolute strain measurements with a high sensitivity, thus opening a door for new possibilities which are yet to be explored.

Keywords: fiber optics sensor; Rayleigh scattering; Brillouin scattering; fast measurement

Wang B Z, Ba D X, Chu Q, Qiu L Q, Zhou D W et al. High-sensitivity distributed dynamic strain sensing by combining Rayleigh and Brillouin scattering. *Opto-Electron Adv* 3, 200013 (2020).

Introduction

The fluctuations of optical properties result in light scattering in the optical fiber, the mechanisms of which can be classified into three major categories, known as the Rayleigh scattering, Brillouin scattering and Raman scattering¹. Rayleigh scattering is a typical quasi-elastic scattering resulting from the non-propagating density fluctuations, introducing no frequency shift to the scattering wave. Brillouin scattering is the light scattering from the density waves (i.e. acoustic phonons), adding a Doppler

shift to its backscattering wave. Raman scattering is generated by the transition of medium molecules in vibrational and rotational modes, which can be described as the scattering of light from the optical phonons. The optical properties in the fiber fluctuate with the environmental disturbances, which influence the intensity or frequency shift of scattering waves¹. In the past 40 years, the scattering based optical fiber sensors have been widely investigated, where the common communication fiber allows for distributed measurements with low loss and high sensitivity. In 1976,

National Key Laboratory of Science and Technology on Tunable Laser, Harbin Institute of Technology, Harbin 150001, China.

[†]These authors contributed equally to this work.

*Correspondence: Y K Dong, E-mail: aldendong@163.com

Received: 23 April 2020; Accepted: 2 July 2020; Published: 24 December 2020

200013-1

the first distributed optical fiber sensing scheme was reported, known as the optical time-domain reflectometry (OTDR), which has been well commercialized and widely used to investigate the fiber attenuation characteristics². In 1980s, a distributed optical fiber temperature sensor was demonstrated based on the Raman scattering³, while the Brillouin frequency shift (BFS) has been measured for distributed temperature and strain sensing^{4,5}. At present, both the Rayleigh and Brillouin based sensors allow for the strain and temperature measurements, and their applications range from structure health monitoring to geophysical exploration.

The phase-sensitive OTDR (φ -OTDR) and Brillouin optical time domain analysis (BOTDA) are typical time-domain systems, in which the optical pulse is employed for distributed sensing. In recent twenty years, great advances in devices and schemes have promoted the improvements on the performances of distributed optical fiber sensors, especially in the aspects of long range⁶⁻⁸, high spatial resolution^{9,10}, high accuracy^{11,12}, dynamic measurements¹³⁻¹⁷ and multi-parameter sensing^{18,19}. For the simplest implementation of φ -OTDR, a highly coherent light source is pulse modulated to interrogate the sensing fiber²⁰. The intensity trace of the Rayleigh scattering signal is measured with a jagged shape, as a consequence of the coherent interference among a large number of Rayleigh scattering centers. The temperature or strain variation on the sensing fiber causes the change of optical path between different scattering centers (i.e. phase changes for the light), resulting in a modification on the coherent superposition of Rayleigh scattering light. Furthermore, several promising techniques have been proposed for the phase recovery to enable the quantitative measurements, including the frequency-controlled light source²¹, Michelson interferometer²², coherent detection^{14,23,24}, dual-wavelength pulses²⁵, and chirped pulses^{26,27} etc. By using the pulse-to-pulse frequency-scanning method, the local Rayleigh spectrum can be mapped, where the optical phase change manifests itself as a frequency shift of the intensity distribution²¹. The correlation between the measured and the reference spectra generates a correlation peak at a frequency detuning, and it is proportional to the temperature and strain variations²¹. Based on the correlation between two orthogonal polarization spectra, the frequency-scanning φ -OTDR allows for distributed birefringence and hydrostatic pressure measurements^{28,29}. In order to realize the fast measurements, the wavelength scanning is enabled by

using the laser current modulation with a saw-tooth signal³⁰.

However, the frequency-scanning φ -OTDR is more suitable for high-sensitivity relative strain measurements rather than absolute strain demodulation. Because the absolute strain is obtained by accumulating the relative strain change between two continuous measurements, the monitoring process is required to be made continuously and start with no strain applied. Moreover, the measurement errors are introduced and then accumulated during the data processing, which degrades the measurement accuracy¹². Fortunately, the BOTDA can provide high-accuracy absolute strain information by using the BFS³¹, while it is not able to realize nano-strain measurements due to its low strain resolution. For the fast Brillouin sensing, several impressive technologies have been proposed to expedite the measurement speed, such as the optical frequency comb technique^{32,33}, slope-assisted method^{13,34}, frequency-agile technique³¹, optical frequency division multiplexing technique^{35,36}, and optical chirp chain technique³⁷. Based on the above analysis, both the φ -OTDR and BOTDA sensors are able to realize the dynamic strain measurements, but the intended applications are different for these two sensors. In 2017, a space-division multiplexed hybrid φ -OTDR and BOTDA system has been proposed, which allows ultra-high measurement resolution (0.001 μm) and large dynamic range (10 m)³⁸. As a result, they are complementary schemes rather than substitutes for each other, so that the cooperation can extend the functions and explore new application areas. However, the frequency-scanning operation is performed on two different modulators and the signals of BOTDA and φ -OTDR are collected in different cores of the multi-core fiber, which increases the complexity of the system.

In this paper, we demonstrate high-sensitivity distributed dynamic strain measurements by combining the Rayleigh and Brillouin sensing. These two sensing signals are collected simultaneously with the same set of frequency-scanning optical pulses. The article is organized in the following manner: Section 2 describes the principle of the proposed sensor and the experiment setup is shown in Section 3. Then, the performance of the proposed sensor is investigated by an elaborate experiment, where a 9.9 Hz vibration under two absolute strains has been measured with a high sensitivity of 6.8 ne. The experiment results and discussions are provided in Section 4, and finally Section 5 makes the conclusion.

Principles

In the φ -OTDR system, the frequency of the optical pulse is scanned to map the Rayleigh spectrum. Similarly, the frequency scanning is also the critical process in the BOTDA scheme to reconstruct the Brillouin gain spectrum (BGS). Therefore, it is feasible to simultaneously measure the φ -OTDR and BOTDA signals by using the same set of frequency-scanning optical pulses. As shown in Fig. 1(a), the frequency-scanning optical pulses are obtained by two steps. First, the frequency of the optical wave is scanned from ν_1 to ν_N by using the frequency-agile technique, so that the frequency switching time can be ignored^{31,39}. Moreover, the lasting time of each frequency wave is T , and then the optical wave is pulse modulated in each frequency duration. After obtaining the frequency-scanning optical pulses, they enter into the fiber under test (FUT) in sequence as depicted in Fig. 1(b), and only one pulse travels in the FUT to avoid the signal overlapping. The probe wave for BOTDA sensing is injected from the other end of the sensing fiber, which travels in the same direction as the Rayleigh scattering signal.

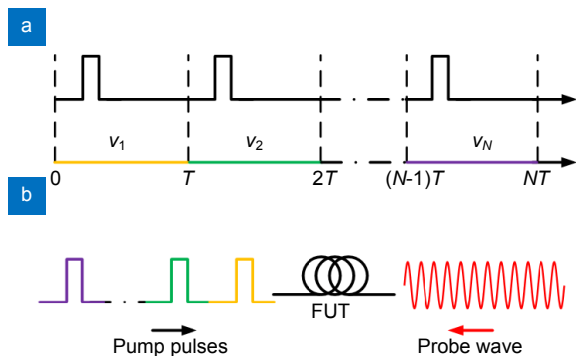


Fig. 1 | (a) Two modulation steps to obtain the frequency-scanning optical pulses. (b) The sequence diagram of the pump pulses and probe wave.

Next, the Rayleigh and Brillouin signals are collected at the same end of the FUT, and the frequency relationship of which is shown in Fig. 2. Here, ν_0 is the frequency of the probe wave, and the frequency range of optical pulses is wide enough to map the Rayleigh and Brillouin spectra. It should be noted that the frequency offset between the pump pulse and probe wave should be scanned in the vicinity of the fiber BFS. The frequency of Rayleigh scattering signals is equal to that of the optical pulse, so that it is able to separate Rayleigh scattering from probe signals according to the frequency difference. A fiber Bragg grating (FBG) is used to reflect the Rayleigh scattering signal,

and meanwhile the probe wave passes through the FBG. Alternatively, it is also able to collect the Rayleigh scattering through the transmission passband of the FBG, and the probe wave is reflected by the FBG. For this scheme, every set of the frequency-scanning pulses can be regarded as one sampling to the vibration on the fiber, and therefore, the sampling rate to the vibration is equivalent to the repetition rate of pump pulse sequence. Moreover, the sensing range and spatial resolution is determined by the time interval T and pulse width, respectively.

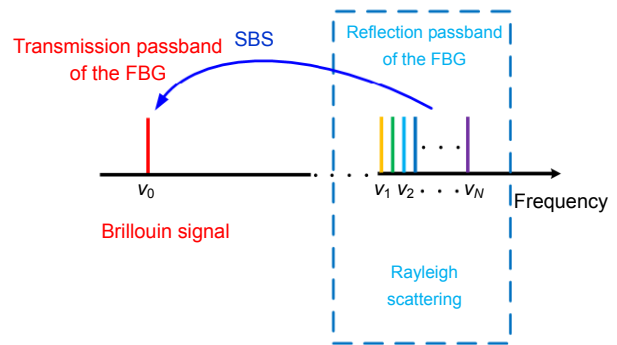


Fig. 2 | The frequency relationship between the Rayleigh scattering and Brillouin signals.

The Rayleigh spectrum is simulated with a frequency scanning of 1 GHz, using the one-dimensional impulse-response model²¹. As shown in Fig. 3(a), the reference spectrum is drawn in the black short dash line, while the red line corresponds to the measured spectrum. Then, the optical frequency change $\Delta\nu_m$ can be computed using the cross-correlation algorithm between these two Rayleigh spectra. Furthermore, strain change $\Delta\varepsilon$ and temperature change ΔT can be demodulated according to the following formula^{21,25,30}:

$$\frac{\Delta\nu_m}{\nu_1} = K_\varepsilon \Delta\varepsilon + K_T \Delta T, \tag{1}$$

where the K_ε and K_T are the strain and temperature coefficients in the φ -OTDR scheme, respectively.

With the same frequency range, the Brillouin gain spectra of the initial and final states are plotted in Fig. 3(b). The initial state of the strain ε_0 and temperature T_0 is given for the FUT, and the corresponding BGS is plotted in black short dash line. In the final state, the BGS is exhibited in the red solid line, and moreover the absolute strain ε and temperature T can be obtained using the Equation (2)⁴⁰:

$$\nu_B - \nu_{B0} = C_\varepsilon (\varepsilon - \varepsilon_0) + C_T (T - T_0), \tag{2}$$

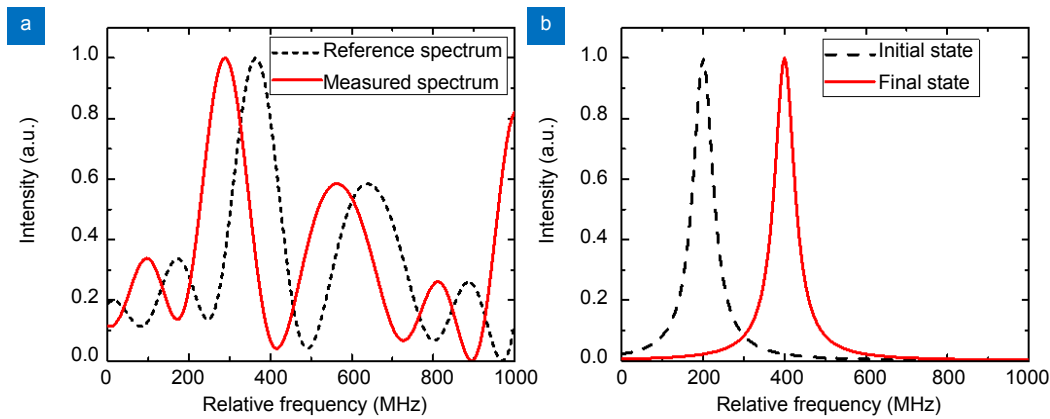


Fig. 3 | (a) Simulated Rayleigh intensity distribution along 1 GHz frequency span: reference spectrum (black short dash line) and measured spectrum (red line). (b) The BGSs of the initial state (black short dash line) and final state (red solid line).

where ν_{B0} and ν_B are the initial and final BFS of the FUT; C_ϵ and C_T are the strain and temperature coefficient in the Brillouin sensing, respectively.

Experimental setup

As a verification of the proposed scheme, the experiment setup was implemented as shown in Fig. 4. It was basically a classical fast-BOTDA scheme, where, in this case, an additional photo-detector (PD) was used to collect the Rayleigh scattering signal. The light source was an ultra-narrow-linewidth laser (laser1), which was operated at the wavelength of 1550 nm. The laser output was split into two divisions with a 90/10 optical coupler. The 10% division served as the probe wave for the BOTDA measurement, the power of which was adjusted by a variable optical attenuator (VOA) to 100 μ W. The other 90% light was used to generate the frequency-agile modulated pump pulses. An electro-optic modulator (EOM1) was biased at the minimum transmission point to generate two first-order sidebands with suppressed carrier. And the driving microwave signal was provided by the channel 1 (CH1) of the arbitrary waveform generator (AWG), sweeping from 10.6 GHz to 11.1 GHz with a frequency step of 4 MHz. Therefore, there were 126 frequency components in one temporal frame, and the lasting time of each frequency was 0.78 μ s, which allows for a maximum measurement range of 78 m. In order to obtain a flat power distribution after the frequency modulation, an injection-locking scheme was utilized, where another laser (laser2) served as the slave laser. The upper-sideband of the input light was selected by tuning the current and temperature of the slave laser. Then, the EOM2 was also operated at the minimum transmission point for 20 ns pulse modulation, and the electric pulses

were offered by the CH2 of the AWG. As a result, the spatial resolution of 2 m was obtained for both ϕ -OTDR and BOTDA measurements. The peak power of frequency-agile modulated pump pulses was amplified to 500 mW by EDFA1.

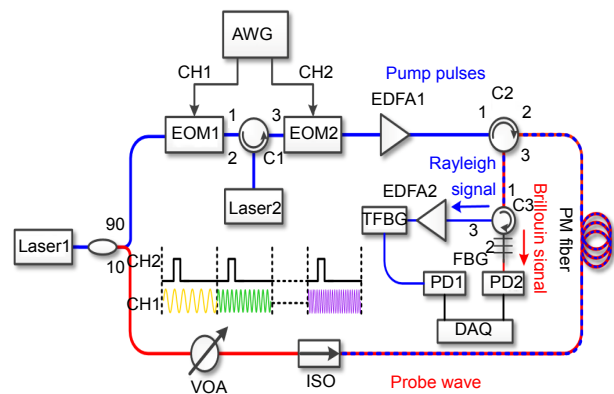


Fig. 4 | The experiment setup of the proposed sensor by combining the Rayleigh and Brillouin measurements.

The lasting time of one set of pump sequence was 98.28 μ s (126 \times 0.78 μ s) and the time interval between two pump sequence was elaborately designed to be 1.72 μ s, resulting in a maximum sampling rate of 10 kHz with no averaging. Next, the pump pulses were injected into the polarization-maintaining (PM) fiber through an optical circulator (C2), so that the SBS interaction is free from the polarization induced fluctuations. The Rayleigh and the Brillouin signals were collected through Port3 of the C2. Then, they were separated by C3 and FBG, where only the Rayleigh scattering signal was reflected by the FBG. After the separation, the Rayleigh signal was amplified by the EDFA2, and the amplified spontaneous emission noise was suppressed by a tunable FBG (TFBG). Next, a high-gain PD1 with 100 MHz bandwidth was used for the detection of

Rayleigh signal, while a 350 MHz PD2 was employed to detect the Brillouin signal. Both the Rayleigh and Brillouin signals carried the strain information applied to the FUT, and the output of these two PDs was simultaneously recorded by a dual-channel data acquisition (DAQ) with 1 GSa/s sampling rate.

Results and discussions

In the experiment, a 2-m fiber segment of the 50-m PM fiber was stretched tight, which was located at the position between 42 m and 44 m, and one end of the fiber was fixed on a motorized positioning system. By applying a relative sub-micron displacement, the distributed correlation spectra along the FUT were shown in Fig. 5(a), which were computed by the measured Rayleigh spectra before and after applying the relative sub-micro strain. It could be seen that the frequency shift was zero at the positions with no strain change, while a frequency shift was measured at the position between 42 m and 44 m. Here, only the relative strain change was demodulated, as the fixed strain had already been applied before the system running. Fortunately, the Brillouin signals were also recorded simultaneously and the top-view of 3-D BGSs were shown in Fig. 5(b). At the position between 42 m and 44 m, the peak of the BGSs was moved comparing with the BGSs without strain, so that the pre-applied strain could be demodulated. In this case, the Brillouin sensing could provide the absolute strain as a reference.

In order to realize the quantitative measurements, the strain coefficients of the Rayleigh and Brillouin sensing were measured, respectively. In the Rayleigh measurements, the displacement of the motorized positioning system was moved from 0 μm to 2 μm with a step of 0.2 μm . The Rayleigh spectra were recorded as a function of time, and the 3-D Rayleigh spectra were shown in Fig.

6(a). In order to reduce the environmental disturbance induced noise, the whole measurement of the Rayleigh strain coefficient was made within 0.7 s. The frequency shift of the intensity distribution was provided in Fig. 6(b), and the linear fitting result was also plotted in red line. As a result, the strain coefficient K_ϵ was obtained, the value of which was -148 MHz/ $\mu\epsilon$. For the BOTDA measurements, a new positioning platform was used to provide a wide strain dynamic range. The BGSs were measured from 220 $\mu\epsilon$ to 3970 $\mu\epsilon$, as shown in Fig. 6(c). The Lorentz-curve fitting method was employed to extract the BFS, the result of which was drawn in Fig. 6(d). The Brillouin strain coefficient C_ϵ was 0.0462 MHz/ $\mu\epsilon$, which was obtained by the linear fitting method.

To demonstrate the sensor capability of high-sensitivity dynamic strain measurements, a vibration was applied to the FUT by changing the motorized positioning system between the two positions periodically, and the relative displacement was 1 μm , corresponding to 500 n ϵ . Moreover, a fixed large strain was applied in advance, and two groups of experiments were made with the same vibration under different absolute strains. In order to increase the recording time to 1 s, the repetition rate of one set of optical pulses was reduced to 1 kHz. As shown in Fig. 7(a), the Brillouin demodulation results of these two groups were provided with 5 moving average, while the fiber without strain was used as a reference. It could be seen that the Brillouin signals showed the absolute strain change between two groups of measurements, but the sub-micro strain vibration was failed to be measured due to the relative low strain resolution. The average absolute strains of these two groups were 296.7 $\mu\epsilon$ and 554.8 $\mu\epsilon$, respectively. The measurement accuracy of the absolute strain was about 5.4 $\mu\epsilon$, computed by the standard deviation of reference fiber BFS. The ϕ -OTDR demodulation

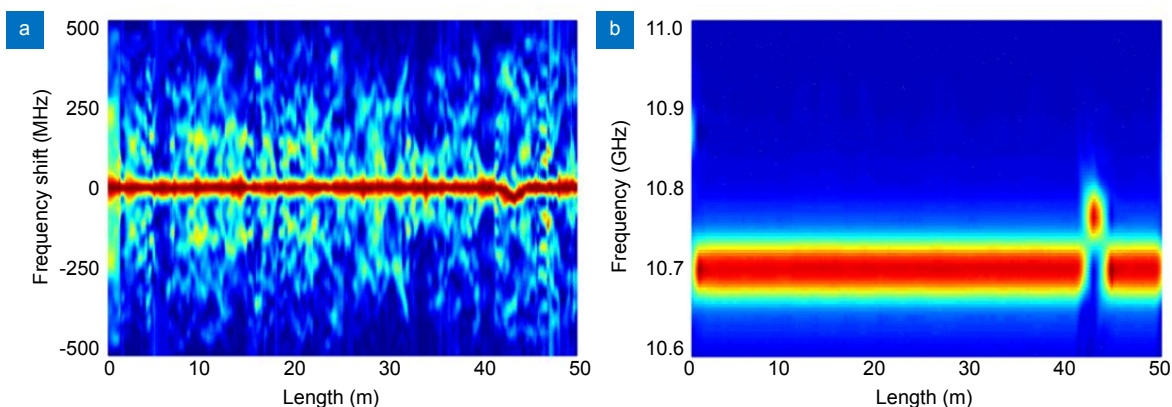


Fig. 5 | (a) The cross-correlation between Rayleigh spectra along the FUT containing the relative sub-micro strain information. (b) The measured 3-D BGSs along the FUT, showing the pre-applied strain information.

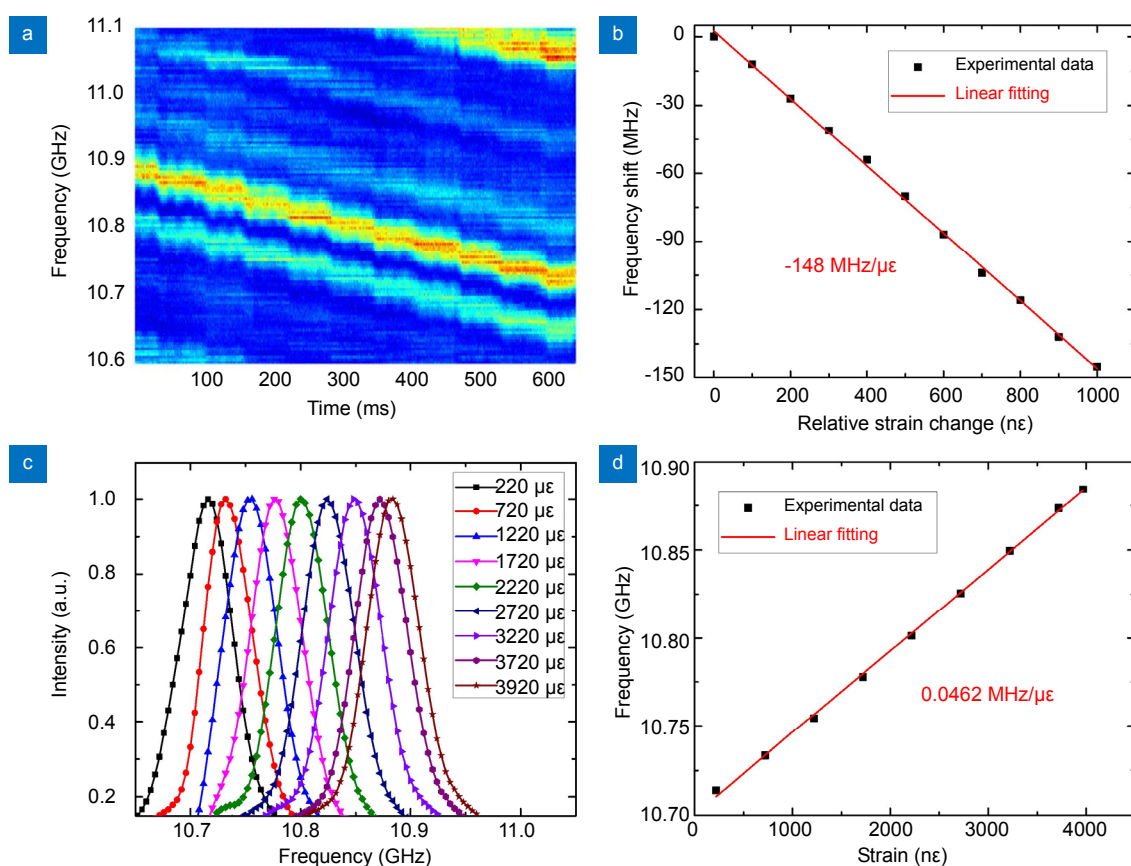


Fig. 6 | (a) The measured Rayleigh spectra recording a 1000 nε relative strain change with a step of 100 nε. (b) The frequency shift in different relative strain change and its linear fitting result. (c) The measured BGSs at different strains from 220 με to 3970 με. (d) The BFS in different strains and its linear fitting result.

results were shown in Figs. 7(b) and 7(c) with no averaging, and the frequency resolution of the correlation was improved to 1 MHz by using the interpolation approach³⁰. A 9.9 Hz vibration with a peak-to-peak value of 500 nε was obtained, but these two dynamic strain results were similar containing only the information of relative strain variations. By combining the Rayleigh and Brillouin measurement results, the dynamic strain changed in the range from 296.45 με to 296.95 με periodically, as displayed by the right y-coordinate of Fig. 7(b). Similarly, the dynamic strain of Group2 varied between 554.55 με and 555.05 με. The standard deviation of the fiber correlation spectra with no strain was less than half of the frequency resolution, so that it was safe to define the sensor relative strain accuracy to be 6.8 nε by the frequency resolution (1 MHz). It could be seen that the proposed sensor was able to provide a high-sensitivity (6.8 nε) dynamic absolute strain results by combining the Rayleigh and Brillouin information.

Besides, the Rayleigh and Brillouin signals are obtained simultaneously using the same set of frequency-scanning

pulses, which does not increase the complexity of the proposed sensor.

Conclusion

In this work, the high-sensitivity distributed dynamic strain measurements have been experimentally demonstrated by combining the Rayleigh and Brillouin sensing, the signals of which are collected simultaneously with the same set of frequency-scanning optical pulses. In the experiment, a vibration of ±250 nε has been measured twice under different absolute strain (296.7 με and 554.8 με). The sub-micro strain vibration is demonstrated by the φ-OTDR signal with a high sensitivity of 6.8 nε, while the absolute strain change is measured by the BOTDA signal with 5.4 με measurement accuracy. Both the φ-OTDR and BOTDA sensors are not able to finish this work alone, while the proposed sensor allows for high-sensitivity dynamic strain measurements. Furthermore, the research of dual-mechanism (Rayleigh and Brillouin) sensing is only in its infancy, so more possibilities and applications are expected in the future.

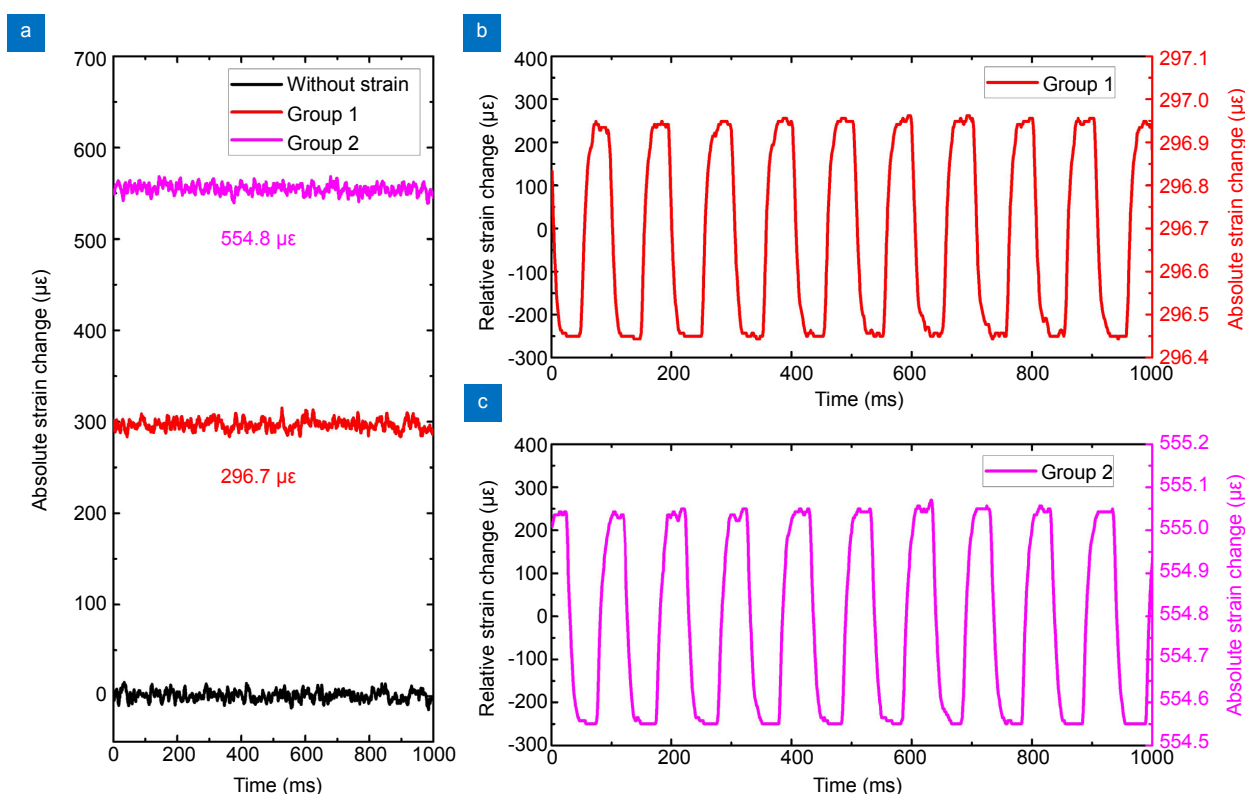


Fig. 7 | Two groups of vibration measurements by integrating the Rayleigh and Brillouin strain information. (a) The dynamic strain measurement results of two groups using the BOTDA. (b, c) The dynamic strain measurement results of the group 1 (b) and group 2 (c) employing the Φ -OTDR, respectively.

Reference

- Boyd R W. *Nonlinear Optics* 3rd ed (Academic Press, Amsterdam, 2008).
- Barnoski M K, Jensen S M. Fiber waveguides: a novel technique for investigating attenuation characteristics. *Appl Opt* **15**, 2112–2115 (1976).
- Dakin J P, Pratt D J, Bibby G W, Ross J N. Distributed optical fibre Raman temperature sensor using a semiconductor light source and detector. *Electron Lett* **21**, 569–570 (1985).
- Culverhouse D, Farahi F, Pannell C N, Jackson D A. Potential of stimulated Brillouin scattering as sensing mechanism for distributed temperature sensors. *Electron Lett* **25**, 913–915 (1989).
- Horiguchi T, Kurashima T, Tateda M. Tensile strain dependence of Brillouin frequency shift in silica optical fibers. *IEEE Photonics Technol Lett* **1**, 107–108 (1989).
- Wang B Z, Fan B H, Zhou D W, Pang C, Li Y et al. High-performance optical chirp chain BOTDA by using a pattern recognition algorithm and the differential pulse-width pair technique. *Photonics Res* **7**, 652–658 (2019).
- Peng F, Wu H, Jia X H, Rao Y J, Wang Z N et al. Ultra-long high-sensitivity Φ -OTDR for high spatial resolution intrusion detection of pipelines. *Opt Express* **22**, 13804–13810 (2014).
- Wang B Z, Pang C, Zhou D W, Dong Y K. Advances of key technologies in long-range distributed Brillouin optical fiber sensing. *Opto-Electron Eng* **45**, 170484 (2018).
- Wang B Z, Dong Y K, Ba D X, Bao X Y. High spatial resolution: an integrative review of its developments on the Brillouin optical time- and correlation-domain analysis. *Meas Sci Technol* **31**, 052001 (2020).
- Lu B, Pan Z Q, Wang Z Y, Zheng H R, Ye Q et al. High spatial resolution phase-sensitive optical time domain reflectometer with a frequency-swept pulse. *Opt Lett* **42**, 391–394 (2017).
- Lin W Q, Yang Z S, Hong X B, Wang S, Wu J. Brillouin gain bandwidth reduction in Brillouin optical time domain analyzers. *Opt Express* **25**, 7604–7615 (2017).
- Zhang L, Costa L, Yang Z S, Soto M A, Gonzalez-Herraez M et al. Analysis and reduction of large errors in rayleigh-based distributed sensor. *J Lightw Technol* **37**, 4710–4719 (2019).
- Ba D X, Wang B Z, Zhou D W, Yin M J, Dong Y K et al. Distributed measurement of dynamic strain based on multi-slope assisted fast BOTDA. *Opt Express* **24**, 9781–9793 (2016).
- Dong Y K, Chen X, Liu E H, Fu C, Zhang H Y et al. Quantitative measurement of dynamic nanostrain based on a phase-sensitive optical time domain reflectometer. *Appl Opt* **55**, 7810–7815 (2016).
- Shao L Y, Liu S Q, Bandyopadhyay S, Yu F H, Xu W J et al. Data-driven distributed optical vibration sensors: a review. *IEEE Sens J* **20**, 6224–6239 (2020).
- He H J, Shao L Y, Luo B, Li Z L, Zou X H et al. Multiple vibrations measurement using phase-sensitive OTDR merged with Mach-Zehnder interferometer based on frequency division multiplexing. *Opt Express* **24**, 4842–4855 (2016).
- Peng F, Duan N, Rao Y J, Li J. Real-time position and speed monitoring of trains using phase-sensitive OTDR. *IEEE Photonics Technol Lett* **26**, 2055–2057 (2014).
- Zhang J D, Zhu T, Zhou H, Huang S H, Liu M et al. High spatial resolution distributed fiber system for multi-parameter sensing based on modulated pulses. *Opt Express* **24**, 27482–27493

- (2016).
19. Zhao Z Y, Tang M, Lu C. Distributed multicore fiber sensors. *Opto-Electron Adv* **3**, 190024 (2020).
 20. Juarez J C, Maier E W, Nam Choi K, Taylor H F. Distributed fiber-optic intrusion sensor system. *J Lightw Technol* **23**, 2081–2087 (2005).
 21. Koyamada Y, Imahama M, Kubota K, Hogari K. Fiber-optic distributed strain and temperature sensing with very high measurand resolution over long range using coherent OTDR. *J Lightw Technol* **27**, 1142–1146 (2009).
 22. Wang C, Wang C, Shang Y, Liu X H, Peng G D. Distributed acoustic mapping based on interferometry of phase optical time-domain reflectometry. *Opt Commun* **346**, 172–177 (2015).
 23. Wang Z N, Zhang L, Wang S, Xue N T, Peng F et al. Coherent Φ -OTDR based on I/Q demodulation and homodyne detection. *Opt Express* **24**, 853–858 (2016).
 24. He H J, Shao L Y, Li Z L, Zhang Z Y, Zou X H et al. Self-mixing demodulation for coherent phase-sensitive OTDR system. *Sensors* **16**, 681 (2016).
 25. Liehr S, Muanenda Y S, Münzenberger S, Krebber K. Relative change measurement of physical quantities using dual-wavelength coherent OTDR. *Opt Express* **25**, 720–729 (2017).
 26. Pastor-Graells J, Martins H F, Garcia-Ruiz A, Martin-Lopez S, Gonzalez-Herraez M. Single-shot distributed temperature and strain tracking using direct detection phase-sensitive OTDR with chirped pulses. *Opt Express* **24**, 13121–13133 (2016).
 27. Bhatta H D, Costa L, Garcia-Ruiz A, Fernandez-Ruiz M R, Martins H F et al. Dynamic measurements of 1000 microstrains using chirped-pulse phase-sensitive optical time-domain reflectometry. *J Lightw Technol* **37**, 4888–4895 (2019).
 28. Soto M A, Lu X, Martins H F, Gonzalez-Herraez M, Thévenaz L. Distributed phase birefringence measurements based on polarization correlation in phase-sensitive optical time-domain reflectometers. *Opt Express* **23**, 24923–24936 (2015).
 29. Mikhailov S, Zhang L, Geernaert T, Berghmans F, Thevenaz L. Distributed hydrostatic pressure measurement using Phase-OTDR in a highly birefringent photonic crystal fiber. *J Lightw Technol* **37**, 4496–4500 (2019).
 30. Liehr S, Münzenberger S, Krebber K. Wavelength-scanning coherent OTDR for dynamic high strain resolution sensing. *Opt Express* **26**, 10573–10588 (2018).
 31. Peled Y, Motil A, Tur M. Fast Brillouin optical time domain analysis for dynamic sensing. *Opt Express* **20**, 8584–8591 (2012).
 32. Chaube P, Colpitts B G, Jagannathan D, Brown A W. Distributed fiber-optic sensor for dynamic strain measurement. *IEEE Sens J* **8**, 1067–1072 (2008).
 33. Voskoboinik A, Yilmaz O F, Willner A W, Tur M. Sweep-free distributed Brillouin time-domain analyzer (SF-BOTDA). *Opt Express* **19**, B842–B847 (2011).
 34. Bernini R, Minardo A, Zeni L. Dynamic strain measurement in optical fibers by stimulated Brillouin scattering. *Opt Lett* **34**, 2613–2615 (2009).
 35. Zhao C, Tang M, Wang L, Wu H, Zhao Z Y et al. BOTDA using channel estimation with direct-detection optical OFDM technique. *Opt Express* **25**, 12698–12709 (2017).
 36. Fang J, Xu P B, Dong Y K, Shieh W. Single-shot distributed Brillouin optical time domain analyzer. *Opt Express* **25**, 15188–15198 (2017).
 37. Zhou D W, Dong Y K, Wang B Z, Pang C, Ba D X et al. Single-shot BOTDA based on an optical chirp chain probe wave for distributed ultrafast measurement. *Light Sci Appl* **7**, 32 (2018).
 38. Dang Y L, Zhao Z Y, Tang M, Zhao C, Gan L et al. Towards large dynamic range and ultrahigh measurement resolution in distributed fiber sensing based on multicore fiber. *Opt Express* **25**, 20183–20193 (2017).
 39. Wang B Z, Hua Z J, Pang C, Zhou D W, Ba D X et al. Fast Brillouin optical time-domain reflectometry based on the frequency-agile technique. *J Lightw Technol* **38**, 946–952 (2020).
 40. Horiguchi T, Shimizu K, Kurashima T, Tateda M, Koyamada Y. Development of a distributed sensing technique using Brillouin scattering. *J Lightw Technol* **13**, 1296–1302 (1995).

Acknowledgements

This work was supported by the National Key Scientific Instrument and Equipment Development Project of China (2017YFF0108700) and National Natural Science Foundation of China (61975045). The authors would like to express our gratitude to Long Wang, Chao Pang and Yabo Feng for their help in the experiment.

Competing interests

The authors declare no competing financial interests.